3-27-2023

Deeper habitats and cooler temperatures moderate a climate-driven seagrass disease

Olivia J. Graham
Cornell University

Tiffany Stephens
Seagrove Kelp Co

Brendan Rappazzo
Cornell University

Corinne Klohmann
Cornell University

Sukanya Dayal
Cornell University

See next page for additional authors

Recommended Citation

Olivia J. Graham, Tiffany Stephens, Brendan Rappazzo, Corinne Klohmann, Sukanya Dayal, Emily M. Adamczyk, Angeleen Olson, Margot Hessing-Lewis, Morgan Eisenlord, Bo Yang, Colleen Burge, Carla P. Gomes, and Drew Harvell. "Deeper habitats and cooler temperatures moderate a climate-driven seagrass disease" *Philosophical Transactions of the Royal Society B: Biological Sciences* (2023). https://doi.org/10.1098/rstb.2022.0016

PHILOSOPHICAL TRANSACTIONS
OF THE ROYAL SOCIETY B
BIOLOGICAL SCIENCES

Deeper habitats and cooler temperatures moderate a climate-driven disease in an essential marine habitat

Journal:	*Philosophical Transactions B*
Manuscript ID	Draft
Article Type:	Research
Date Submitted by the Author:	n/a
Complete List of Authors:	Graham, Olivia J.; Cornell University, Department of Ecology and Evolutionary Biology Stephens, Tiffany; Seagrove Kelp Co Rappazzo, Brendan; Cornell University, Computer Science Klohmann, Corinne; Cornell University, Ecology and Evolutionary Biology; University of Washington, School of Aquatic and Fishery Sciences Dayal, Sukanya; Cornell University, Natural Resources; University of North Carolina Wilmington, Biology and Marine Biology Adamczyk, Emily; The University of British Columbia, Department of Zoology and Biodiversity Research Centre Olson, Angeleen M.; Hakai Institute Hessing-Lewis, Margot; Hakai Institute Eisenlord, Morgan; Cornell University, Ecology and Evolutionary Biology Yang, Bo; San Jose State University, Urban and Regional Planning Burge, Colleen; University of Maryland Baltimore County, Institute of Marine and Environmental Technology; University of Maryland Baltimore, Department of Microbiology and Immunology; California Department of Fish & Wildlife, University of California Davis Bodega Marine Laboratory Gomes, Carla; Cornell University, Department of Computer Science Harvell, Drew; Cornell University, Ecology and Evolutionary Biology
Issue Code (this should have already been entered and appear below the blue box, but please contact the Editorial Office if it is not present):	DISEVOL
Subject:	Ecology < BIOLOGY, Health and Disease and Epidemiology < BIOLOGY
Keywords:	seagrass, eelgrass, marine disease, seagrass wasting disease, climate change, climate refugia

Author-supplied statements

Relevant information will appear here if provided.

Ethics

Does your article include research that required ethical approval or permits?:
This article does not present research with ethical considerations

Statement (if applicable):
CUST_IF_YES_ETHICS :No data available.

Data

It is a condition of publication that data, code and materials supporting your paper are made publicly available. Does your paper present new data?:
Yes

Statement (if applicable):
1. For initial submission, I am happy to share my data and code with reviewers via a shared Google Drive, Box folder, or other method, as preferred. As I am still curating the data (cleaning code, preparing metadata files, etc.), I do not currently have these uploaded to Cornell's eCommons Repository, but will share complete, polished versions by the time of publication.

2. On revision: All data and R scripts used to generate the analyses presented here will be publicly available via the Cornell University eCommons Repository by the time of publication (https://doi.org/10.7298/6ybh-w566).

Conflict of interest

I/We declare we have no competing interests

Statement (if applicable):
CUST_STATE_CONFLICT :No data available.

Title

Deeper habitats and cooler temperatures moderate a climate-driven disease in an essential marine habitat

Authors

Olivia J. Graham[1]*, Tiffany Stephens[2], Brendan Rappazzo[3], Corinne Klohmann[1], Sukanya Dayal[4,5], Emily M. Adamczyk[6], Angeleen Olson[7], Margot Hessing-Lewis[7], Morgan Eisenlord[1], Bo Yang[8], Colleen Burge[9,10,a], Carla P. Gomes[3], Drew Harvell[1]

Affiliations

[1]Department of Ecology and Evolutionary Biology, Cornell University, Ithaca, NY
[2]Seagrove Kelp Co, Ketchikan AK
[3]Department of Computer Science, Cornell University, Ithaca, NY
[4]Department of Natural Resources, Cornell University, Ithaca, NY
[5]Department of Biology and Marine Biology, University of North Carolina, Wilmington, NC
[6]Department of Zoology and Biodiversity Research Centre, University of British Columbia, Unceded xʷməθkʷəy̓əm (Musqueam) Territory, Vancouver, BC
[7]Hakai Institute, Calvert Island, BC
[8]Department of Urban and Regional Planning, San Jose State University, San Jose, CA
[9]Institute of Marine and Environmental Technology, University of Maryland Baltimore County, Baltimore, MD
[10]University of Maryland Baltimore, Department of Microbiology and Immunology, Baltimore, MD

[a]Current address: California Department of Fish & Wildlife, University of California Davis Bodega Marine Laboratory, Bodega Bay, CA

Contact Information

*Olivia J. Graham
ojg5@cornell.edu
(505) 301-7781

Abstract

Eelgrass creates critical coastal habitats worldwide and fulfills essential ecosystem functions as a foundation seagrass. Climate warming and disease threaten eelgrass, causing mass mortalities and cascading ecological impacts. Subtidal meadows are deeper than intertidal and are valuable fish nursery grounds that may also provide refuge from the temperature-sensitive seagrass wasting disease. From cross-boundary surveys of 5,761 eelgrass leaves from Alaska to Washington and assisted with a machine-language algorithm, we measured outbreak conditions.

Across summers 2017 and 2018, predicted disease prevalence was nearly 40% lower for subtidal than intertidal leaves; in both tidal zones, disease risk was lower for plants in cooler conditions. Even in the environmentally more stable subtidal meadows, we observed high

disease levels, with half of the sites exceeding 50% prevalence. Models predicted reduced disease prevalence and severity under cooler conditions, confirming a strong interaction between disease and temperature. At both tidal zones, prevalence was lower in more dense eelgrass meadows, suggesting disease is suppressed in healthy, higher density meadows. These results underscore the value of subtidal eelgrass and meadows in cooler locations as refugia, indicate that cooling can suppress disease, and have implications for eelgrass conservation and management under future climate change scenarios.

Keywords
Seagrass, eelgrass, marine disease, seagrass wasting disease, climate change, climate refugia

Introduction

The increasing incidence and severity of disease outbreaks [1–3]—fueled by acute and prolonged warming ocean temperatures [1,4–9]—makes disease ecology on both land and sea a priority in the portfolio of climate change research. Temperature-sensitive pathogens that target marine foundation species like corals and eelgrass (*Zostera marina*), a temperate seagrass species, can be especially devastating, given their pivotal roles in driving marine ecosystem structure and function [7,9–11]. Eelgrass has the largest global distribution of any marine angiosperm, and grows in shallow, coastal areas throughout the northern hemisphere, spanning from Baja, Mexico to Alaska [12]. Seagrass wasting disease, caused by the protist *Labyrinthula zosterae*, is one of the current threats to the health and sustainability of global seagrass meadows [13,14]. The pathogen consumes plant chloroplasts [15], impairs photosynthesis [16], produces distinctive black lesions [17–19], and reduces eelgrass growth and belowground sugar stores in natural meadows [20]. Historical disease outbreaks in the 1930s reduced some eelgrass meadows along the Atlantic coasts by 90% and dramatically altered their structure and function [21,22], reducing waterfowl and invertebrate populations [21,23–25], and altering the water quality in coastal regions [26]. Eelgrass disease outbreaks continue to persist in temperate seas worldwide [9,27–32], and can result not only in local extinctions, but also in the loss of the valuable

ecosystem services eelgrass provides: carbon sequestration, sediment stabilization, water filtration, nutrient cycling, and habitat formation [33–35].

Warming ocean temperatures and wasting disease can independently and synergistically interact and harm eelgrass. Rising temperature, including increased frequency and intensity of marine heat waves [36], is the most prominent global change factor impacting seagrass ecosystems [37,38], which are declining globally [39]. Warmer temperatures are associated with dramatic reductions in eelgrass growth [40,41], net primary production [42], density [8,43], and biomass [44]. Dramatic examples include widespread mortality of eelgrass in the Chesapeake Bay, Virginia [42] and other seagrass in Western Australia [47] from marine heatwaves. Following recent marine heatwaves, shallower, warmer estuaries also had reduced eelgrass biomass compared to deeper, cooler estuaries [45]. Further, warmer temperatures under climate change projections are expected to substantially shift eelgrass ranges northward and increase eelgrass susceptibility to anthropogenic and natural stressors like disease [46].

Along with rising temperatures, seagrass wasting disease is among one of many multiple stressors threatening global seagrass meadows [14,48]. Climate change is predicted to increase disease impacts on eelgrass health and meadow resistance [14]. Certain abiotic conditions—including warm temperatures—were implicated in historic wasting disease outbreaks [26,49,50]. More recently, elevated temperatures [9,27,32] were associated with higher disease levels in natural meadows. Field surveys also suggest wasting disease and warmer temperatures facilitated seagrass declines in Sicily, Italy [27] and North America [9,13,14,32,51]. Lab experiments demonstrate the causative agent, *L. zosterae*, grows faster at warmer temperatures up to 25° C [52,53], though the exact mechanisms underlying this relationship remain unknown [54]. Certain eelgrass biometrics are also associated with greater wasting disease. Field surveys detected

significant, positive correlations between disease metrics and eelgrass leaf area and negative correlations between disease and shoot density [9,29,30]. Many other environmental parameters influence eelgrass health and survival (ex: exposure to waves and desiccation stress, salinity, sediment), though temperature, light, and nutrients are the most important for eelgrass health and productivity [40,55,56]. Despite the growing understanding of the role of climate and other environmental drivers on wasting disease, little is known about factors that lead to better outcomes for natural meadows, such as cooler, higher latitudes or deeper water.

To capture a broad range of environmental conditions, better understand the synergistic effects of climate and disease on this foundation species, and determine the potential for cold, deep refugia, disease surveys spanning a wide latitude and depths in the northern range of eelgrass distribution are essential. Previous studies reported that disease was lower in deeper eelgrass meadows (-4 m mean low low water, -2 to -5 m, respectively) in the San Juan Islands, Washington, and Sweden [29,31]. This suggests the hypothesis that deeper, subtidal eelgrass meadows may provide plants with more favorable climatic conditions—and less favorable conditions for the pathogen—that allow them to persist [57,58]. Similar patterns were found among three species of algae, which had more severe infections in shallower regions compared to those at depth [59]. Refugia from climate change and disease pressure could potentially mitigate local extinctions due to disturbances [58]. Already, deeper habitats serve as refugia from marine heatwaves for seaweeds [60], corals [61], temperate reefs [62], and eelgrass [45]. These examples highlight how deeper marine environments could reduce the impacts of climate change and pathogenic stressors, and exemplify the need to further understand host-pathogen interactions in these environments.

We aimed to test the following hypotheses: (i) Disease is reduced in meadows at higher latitudes with cooler temperatures. (ii) Disease levels are lower in deeper, subtidal eelgrass compared to the more environmentally stressful conditions of shallower, intertidal eelgrass. (iii) Disease is higher in high-density eelgrass meadows, since the disease transmits via direct contact with infected leaves [15]. To address these, we surveyed seagrass wasting disease in eelgrass meadows throughout their northern range from Puget Sound, Washington to Southeast Alaska in the Northeast Pacific to explore how disease varied across eight degrees latitude, tidal zones (intertidal or subtidal), environments, and time. Altogether, we surveyed 5,761 eelgrass leaves from paired, adjacent intertidal and subtidal eelgrass meadows for leaf-specific measurements (leaf area, disease prevalence, and severity) and site-specific biometrics (density and canopy height). Intertidal eelgrass meadows are exposed to more stressful, extremely variable environmental conditions at low tide, including higher temperatures, desiccation, UV stress, and at high latitudes, scouring by sea ice [63,64]. In contrast, deeper, subtidal meadows are constantly submerged and have more stable environmental conditions. Just as environmental conditions can vary dramatically with elevational gradients and influence disease dynamics on land [65]—so too can the environment and disease vary with depth in our oceans. Because intertidal eelgrass is exposed at low tide to greater environmental stressors, it could be more vulnerable to infection in a changing climate. Intertidal environments could also be more conducive to pathogen growth. Given the ecological significance of eelgrass meadows—particularly as fish nursery and feeding grounds [66]—and the relatively little that is known about disease at depth [31], we made investigation of subtidal disease a key research priority in this project.

Methods

Field surveys. We surveyed 19 intertidal and subtidal eelgrass meadows across four geographic regions: Southeast Alaska (AK); British Columbia, Canada (BC); San Juan Islands, Washington (SJ); and Puget Sound, Washington (PS) (Figure 1A, Figure S1, Table S1). Regions spanned sea surface temperature gradients and ranged from urban environments with high human impacts to remote environments with minimal to no development. For example, British Columbia sites were in the Hakai Lúxvbálís Conservancy, the largest marine protected area along coastal British Columbia (BC Parks), while Puget Sound sites in Washington were heavily urbanized, with some adjacent to a wastewater treatment plant and railroads. Surveys occurred in the summers of 2017 and 2018, when disease levels peak in temperate eelgrass [9,28,32,67]. Due to logistical constraints, we had to stagger our sampling periods as such: We surveyed British Columbia in late June, Puget Sound in early July, San Juan Islands in mid-late July, and Alaska in early August. Within a given region, we surveyed all sites on the same low-tide series.

In each region, we surveyed 3-5 paired intertidal and subtidal eelgrass meadows, except in British Columbia where three sites were strictly intertidal or subtidal. The San Juan Islands have a history of wasting disease monitoring [9,29,30] and recent, significant meadow declines [9,68]. For each field survey, we ran three, 20-m transects parallel to shore in the middle of both intertidal and subtidal meadows. We sampled intertidal meadows at low tide and subtidal meadows using SCUBA or snorkeling (Supplemental Video 1). During 2017, we recorded the GPS coordinates at the ends of all intertidal transects for subsequent monitoring in 2018, so that we could compare the same parts of the meadows between years. We tracked subtidal transect locations using GPS coordinates from boats, dive compass headings, and in some cases, anchored subtidal transect markers. At each site, we haphazardly collected 120 intertidal and 60

subtidal leaves (n=40 leaves/transect, n=20 subtidal leaves/transect). Given the constraints of working underwater, the significantly larger size of subtidal eelgrass leaves compared to intertidal leaves, and the greater processing time required to process larger leaves, we collected fewer subtidal leaves. Intertidal meadows were at approximately +1 m and subtidal meadows were at depths ranging from approximately -1.8 to -6 m mean low low water. Because disease susceptibility and levels can vary with the age of eelgrass leaves [29], we standardized our collections to the third-rank (third youngest) leaf from each shoot, following other published approaches [9]. For a subset of sites in British Columbia, San Juan Islands and Puget Sound, we also measured shoot density and canopy height from quadrats at three points along each transect (0, 10, 20 m). Due to logistical constraints, we did not measure density in any subtidal Puget Sound meadows in 2018. We stored all leaves in bags with seawater on ice or in a refrigerator until processing for image analyses.

Disease quantification. In lab, we gently scraped epiphytes from eelgrass leaves using soft, flexible rulers. We scanned eelgrass leaves between two transparency sheets with a Canon CanoScan LiDE 220 scanner at 600 dpi resolution within 24 hours of collection. This created digital images of eelgrass leaves for subsequent leaf area and disease measurements. Given that some subtidal leaves were nearly 3 m long, we scanned only diseased or potentially diseased portions of subtidal leaves for more efficient processing. Consequently, we measured the lengths and widths of each subtidal leaf by hand prior to scanning, and used these to calculate subtidal leaf areas. We scanned entire intertidal leaves, which were smaller than subtidal leaves, and used leaf areas measured by a machine-learning algorithm.

To precisely measure leaf-level disease prevalence and severity, we leveraged the Eelgrass Lesion Image Segmentation Analyzer (EeLISA), a robust algorithm that identified and measured healthy and diseased tissue on all images of scanned eelgrass leaves [9,32,69]. The algorithm calculated disease prevalence (presence/absence of disease) and lesion area for each leaf, along with leaf area estimates for intertidal leaves. Using leaf-level prevalence, we calculated transect- and site-level mean prevalence (proportion of infected individual plants); we calculated severity (proportion of infected leaf area) using lesion and leaf area measurements at leaf, transect, and site-levels. Importantly, this award-winning algorithm was instrumental in enabling us to efficiently and consistently survey disease across a broad, latitudinal scale, as previous methods of measuring disease lesions by hand would have severely limited the scope of our surveys; measuring diseased lesions by hand can take more than 30 minutes for one eelgrass leaf and can be a significant bottleneck for disease analyses [69].

Pathogen confirmation. We confirmed that the black-edged, necrotic lesions we identified as wasting disease were caused by the pathogen *L. zosterae* and asymptomatic, healthy eelgrass did not contain *L. zosterae* using qPCR analyses (n=98 eelgrass leaves tested), following established protocols [9,28,32,70]. Subsequent qPCR analyses of diseased eelgrass from the San Juan Island, WA sites also confirmed the presence of *L. zosterae* [32].

Temperature & salinity data. To determine the relationship between disease and sea surface temperatures, we assessed remote-sensed sea surface temperatures for all sites from January – June 2017 and 2018, following previously published methods [9,32]. Briefly, we extracted Group for High Resolution Sea Surface Temperatures (GHRSST) Level 4, Multi-Scale

Ultra-High Resolution (MUR) daily temperatures for each site from the Jet Propulsion Laboratory OPeNDAP portal [71]. For each site, temperatures were extracted from a 1 x 1 km area over the ocean; these sea surface temperatures were measured at the site-level and did not differentiate between subtidal and intertidal meadows, as our surveys did not extend beyond a 1 x 1 km area at each site.

To evaluate sea surface temperatures relative to each site, we calculated five different temperature anomaly metrics for each month (from January – June 2017 and 2018, respectively), consistent with previous work exploring impacts of temperature anomalies on marine environments [5,6,32]; we did not use absolute temperatures. All temperature metrics were calculated based on the daily, satellite-derived sea surface temperature for each site and the long-term, 17-year mean (2002 – 2018) monthly temperature for the site. The five temperature anomaly metrics included: CDiffMean (cumulative difference between daily temperature and long-term mean), CDiffMeanHeat (cumulative positive difference between daily temperature and long-term mean), CDiffMeanCold (cumulative negative difference between daily temperature and long-term mean), CDiffT90Heat (cumulative positive difference between daily temperature and long-term 90th percentile monthly temperature), CDiffT90Cold (cumulative negative difference between daily temperature and long-term 90th percentile monthly temperature). These temperature anomalies were cumulative temperature differences summed over a one-month period. We restricted temperatures from January – June of 2017 and 2018, since we began our disease surveys in late June of each year, and we did not want to include site temperatures after we had already collected eelgrass. We specifically did not include temperature anomalies for regions sampled after June (AK, SJ, PS) because we wanted to run temperature anomaly models that compared disease across all regions and sites simultaneously, rather than separate, region-

specific models. All temperature metrics from January – June 2017 and January – June 2018 were centered and scaled, then subset by month for subsequent models, described below.

Statistical analyses. We performed all statistical analyses in R version 4.1.2 [72] and visualized data using the packages ggplot, ggpubr, and RcolorBrewer [73–75]. Data exploration and subsequent model fitting and validation were carried out following published protocols [76]. We incorporated remote-sensed sea surface temperatures into models to determine the effects of environment (temperature anomaly) and eelgrass biometrics (leaf area, density) on disease prevalence and severity. We used the *glmmTMB* function in the glmmTMB package to fit binomial generalized linear mixed models for prevalence [77], and the *lmer* function and lme4 package to fit linear mixed effects regression models for severity [78]. Fixed effects in all models included tidal zone (subtidal vs intertidal), year, temperature anomaly, and leaf area, and interactions (detailed below); subsequent models also included eelgrass density. We centered and scaled all numeric fixed effects—leaf area, density, and temperature anomaly—in order for the models to converge. To account for the hierarchical sampling design, we included the random nested effects of region, site, tidal zone, and transect in all models. Our nested design allowed for disease comparisons across broad environmental and spatiotemporal gradients.

Given that some parameters were only measured at a subset of sites for both years, we ran several different models on our data. The most comprehensive prevalence and severity models include data from all sites (n=5761 and n=3457 leaves, respectively; Table S2). Subsequent prevalence and severity models used a subset of the dataset, which included density (n=4090 and n=2549 leaves; Table S3). All data and R scripts used to generate the analyses

presented here will be publicly available via the Cornell University eCommons Repository (https://doi.org/10.7298/6ybh-w566).

Developing leaf area, temperature, and disease models

To determine the best binomial generalized linear mixed model structure for leaf-level prevalence (Table S2), we ran models that included fixed effects of leaf area, tidal zone, year, temperature anomaly, and interactions between some of these terms. We only tested interactions that were biologically meaningful, such as leaf area and tidal zone interactions or leaf area and year interactions, but not tidal zone and year interactions. Such interactions were considered potentially biologically meaningful, since subtidal eelgrass leaves are considerably longer and wider compared to those in intertidal zones [79]. Likewise, leaf area could interact with year, if one year was warmer or cooler than another, since temperature strongly influences eelgrass growth [40,41]. We subset temperature anomaly metrics to the month of March for this stage of model development, as March included a range of temperatures above and below the long-term, historical mean. The best-fit prevalence model structure had the lowest AICc (corrected Akaike Information Criterion) and included the following fixed effects and interactions: tidal zone, year, leaf area, temperature anomaly, leaf area*tidal zone, leaf area*year. We then used this model structure to test subsequent monthly temperature anomaly models, switching out the five different temperature anomaly metrics described above (CDiffMean, CDiffMeanHeat, CDiffMeanCold, CDiffT90Heat, CDiffT90Cold), calculated on a monthly basis from January to June. This allowed us to determine which month's temperature metrics were the best fit for the prevalence model. We used AICc to select the best-fit, leaf-level prevalence model, which

included a March cold temperature anomaly (CDiffMeanCold, n=5761 leaves, Table S2). We validated the model by assessing diagnostic plots made with the DHARMa package [80].

We followed a similar process to develop the linear mixed effects regression model for leaf-level severity (Table S2). Because we used a hurdle model approach for analyzing disease severity, we only included data for leaves with disease and excluded healthy individuals; we also logit-transformed severity since the data were bound between 0 and 1, following established protocols [81]. The best-fit, leaf-level severity model had the lowest AICc and included the following fixed effects and interactions: tidal zone, year, leaf area, temperature anomaly, and leaf area*temperature anomaly. This model included a March cold temperature anomaly (CDiffT90Cold, n=3457 leaves, Table S2). To evaluate the model for normality and homogeneity of residuals, we visually checked diagnostic plots created with the *plot_model* function in the sjPlot package [82].

Developing leaf area, temperature, density, and disease models

We developed additional prevalence and severity models (Table S3) based on the subset of sites for which we had eelgrass density—British Columbia, San Juan Islands, Puget Sound—following the model development and selection process described above. The best-fit, binomial generalized linear mixed model for leaf-level prevalence (Prev Mod 2) included the following fixed effects and interactions: tidal zone, year, leaf area, cold temperature anomaly (CDiffMeanCold) for March, density, leaf area*CDiffMeanCold, CDiffMeanCold *mean density, tidal zone*mean density (n=4090 leaves, Table S3). The best-fit, linear mixed effects regression hurdle model for leaf-level severity (Sev Mod 2) included the following fixed effects and interactions: tidal zone, year, leaf area, temperature anomaly (CDiffMean) for March,

density, year*CDiffMean (n=2549 leaves, Table S3). For this model, we also used a "bobyqa" optimizer to support model convergence. As before, we used DHARMa diagnostic plots and qq-plots to assess respective models [80,82].

Results

Broad disease patterns

Disease was significantly higher in 2018 compared to 2017 (Table S2). Among the four regions, disease prevalence (proportion of infected individual plants) and severity (proportion of tissue infected) increased in all regions in 2018 except for Puget Sound, which had reduced disease (Figure 1B, Figure S2, Table S4). The most dramatic changes in disease between years were in the intertidal. Intertidal prevalence in Alaska shifted from 22.05 ± 2.61% to 61.11 ± 3.08% the subsequent year, and regional severity changed from 1.62 ± 0.34% to 11.22 ± 1.08% (mean ± SE, Figure 1B, Figure S2). Spatially, leaf-level disease prevalence and severity were reduced at higher latitudes compared to lower latitude regions, though disease varied considerably between sites (Figure 1B, Figure S2). This latitudinal gradient was more apparent in the higher-resolution severity data, with Alaska and British Columbia reporting lower disease severity across both years and tidal zones compared to regions further south (Figure 1B).

Prevalence and severity were significantly lower in subtidal meadows compared to the intertidal (glmm and lmer, $p<0.001$, Table S2). When averaged across both years, the mean prevalence for intertidal eelgrass was 66.0 ± 0.79%, compared to 50.4 ± 1.06% among subtidal plants (probability ± SE). At the site-level, disease prevalence ranged from 7.93 ± 3.43% to 100% among intertidal eelgrass and from 8.45 ± 3.32% to 95.23 ± 2.7% among subtidal eelgrass

(mean ± SE, Figure S2). Out of 70 total intertidal and subtidal sampling events across the two years, 41 had a mean prevalence greater than 50%, indicating widespread infection (Figure S2). Differences in severity between tidal zones were even more striking (Figure 1B, Table S2). When averaged across both years, severity for intertidal plants was 10.05 ± 0.27%, compared to 3.12 ± 0.17% among subtidal plants (mean severity ± SE). Site-level disease severity ranged from 0.14 ± 0.096% to 33 ± 1.85% among intertidal eelgrass, compared to 0.054 ± 0.029% to 16.3 ± 2.78% among subtidal eelgrass (mean ± SE, Figure 1B). Of the 70 sampling events, 23 had a mean severity greater than 10% (Figure 1B).

Leaf area, temperature, and disease models

We tested five temperature metrics calculated for each month (January – June) when developing leaf-level prevalence and severity models. Of these, March temperature anomalies were in the best-fit models, based on the lowest AICc. Sea surface temperatures in March 2017 and 2018 varied regionally, with generally colder absolute temperatures in higher-latitude regions (Figure S3). All regions experienced warmer temperatures in March 2018 than March 2017 except for Puget Sound, which was cooler that year (Figure 3A). This coincided with reduced disease prevalence and severity in Puget Sound relative to 2017 (Figure 1B, Figure S2).

Leaf-level, summertime prevalence significantly decreased with cooler March temperatures, as predicted (glmm, $p<0.001$, Table S2). Predicted prevalence decreased with cooler March temperature anomalies (CDiffMeanCold) for both intertidal and subtidal eelgrass (Figure 3B). Other significant predictors for leaf-level prevalence included: tidal zone, year, leaf area, leaf area*tidal zone, and leaf area*year (glmm, $p<0.001$, Table S2). Across both tidal

zones, transect-level disease prevalence was positively associated with cumulative March cold temperature anomalies and leaf areas (Figure 2A, Figure S5).

Similarly, leaf-level severity significantly decreased with cooler March temperatures (lmer, $p<0.001$, Table S2). Among diseased leaves, predicted summertime severity decreased with cumulative, 90th percentile cold March temperature anomalies in subtidal and intertidal eelgrass (Figure S4). Compared to absolute cold temperature anomalies measured on a daily basis, this cold temperature anomaly (CDiffT90Cold) is the accumulation of negative differences between each site's daily temperatures and the long-term 90th percentile mean temperatures for March 2017 and 2018. Other significant predictors of leaf-level severity include tidal zone, year, and leaf area*CDiffT90Cold (lmer, $p<0.001$, Table S2). For intertidal leaves, disease severity was positively associated with cumulative, 90th percentile March cold temperature anomalies and leaf areas, though these associations were not as apparent among subtidal leaves (Figure S5, Figure S6).

Leaf area, temperature, density, and disease models

We measured densities in three of the four surveyed regions: British Columbia, San Juan Islands, and Puget Sound. Short survey times in the remote sites in Alaska precluded density measurements. Mean eelgrass densities varied among sites and tidal zones and between years for several sites (Figure S7). Shoot densities were significantly higher in intertidal meadows compared to subtidal in the San Juan Islands (t-test: $t(178)=4.01$, $p<0.001$) and Puget Sound ($t(103)=2.60$, $p=0.01$), but not in British Columbia (Figure S4; $t(124)=-1.82$, $p=0.07$). At the transect level, low-density intertidal eelgrass had higher disease prevalence and severity compared to eelgrass at higher densities (Figure S8). Changes in mean density in 2018 were not

strongly associated with the prior year mean severity (*data not shown*), suggesting that other factors likely interact with disease to influence eelgrass persistence.

Leaf-level prevalence was significantly, inversely associated with mean shoot density (glmm, $p<0.001$, Table S3). High disease levels were associated with reduced eelgrass densities in both subtidal and intertidal meadows (Figure S8). The best-fit prevalence and density model included the following predictors, all of which were significant: tidal zone, leaf area, year, March cold temperature anomaly (CDiffMeanCold), density, leaf area* CDiffMeanCold, CDiffMeanCold*density, tidal zone*density. Interactions between temperature and density had the most pronounced effect on predicted prevalence at low densities. At low densities, lower predicted disease prevalence was associated with cooler temperatures, while higher predicted prevalence was associated with warmer temperatures (Figure S9). This association was consistent at mean densities, but did not persist at high eelgrass densities.

Leaf-level severity was not significantly associated with mean shoot density (lmer, $p>0.05$, Table S3). The best-fit, hurdle severity model included the following: tidal zone, leaf area, year, March temperature anomaly (CDiffMean), density, year* CDiffMean. There was not a consistent association between March temperature anomaly, eelgrass densities, and predicted severity in 2017 and 2018.

Eelgrass biometrics

Consistent with previous work [79], eelgrass leaves were smaller at shallower depths (Figure S7). Mean canopy height was 599.02 ± 9.99% in intertidal eelgrass and 1068.71 mm ± 14.58% in subtidal eelgrass when averaged across years (mean ± SE, Figure S7). Mean leaf area was also smaller among intertidal eelgrass compared to subtidal eelgrass. Across both years,

mean leaf area was 1935.14 mm^2 ± 24.31% in intertidal eelgrass and 5267.93 mm^2 ± 72.76% in subtidal eelgrass (mean ± SE, Figure S7). When modeled with temperature, leaf area was significantly, positively associated with leaf-level disease prevalence (glmm, $p<0.001$, Figure 3B, Table S2). Although subtidal eelgrass leaves were on average nearly three times larger than intertidal eelgrass, disease prevalence and severity were significantly lower in subtidal plants.

qPCR

We successfully confirmed the presence of *L. zosterae* in 19 out of 49 symptomatic, lesioned eelgrass from British Columbia and Puget Sound using qPCR. All asymptomatic eelgrass tested from these regions were qPCR negative for the pathogen (n=49). We isolated *L. zosterae* from diseased eelgrass in the San Juan Islands to confirm pathogen presence (*data not shown*). Other studies also confirmed *L. zosterae* in diseased eelgrass in the San Juan Islands and Alaska [9,29,30,32,53,83]; these findings support that our visual identification of dark, necrotic lesions were caused by *L. zosterae*.

Discussion

The two study years, 2017 and 2018, captured outbreak conditions of relatively high disease levels across a wide latitude in the northern range of eelgrass, from Puget Sound to Alaska, including some relatively undisturbed, remote locations. Our observed disease prevalence and severity levels are comparable to those documented in other intertidal and subtidal eelgrass meadows in the Northeast Pacific [32], including the San Juan Islands [9], though severity levels are considerably higher than those observed in Sweden [31]. Previous work indicates that in natural meadows, diseased eelgrass can have reduced growth rates and

belowground sugar reserves and lesions can rapidly outpace leaf growth [20]. Thus, the surveyed eelgrass meadows with high disease levels could have compromised growth and potentially survival. Against this backdrop of high disease levels, disease risk varied highly across both latitude and tidal zone. Disease prevalence and severity were reduced at cooler sites, the cooler year, and in higher latitudes. This confirms seagrass wasting disease is among the growing number of temperature-sensitive marine diseases [5,10,32].

Of the temperature metrics tested in prevalence and severity models, March cold temperature anomalies were the best predictors for summertime disease levels. Regions with cooler temperatures that may either kill or slow the growth of *L. zosterae* could have lower summer disease levels. While most regions experienced cooler temperatures and reduced disease in 2017, the exception was a cooler Puget Sound in 2018, which stood out as reflecting a temperature-disease association. Disease prevalence and severity were markedly lower in Puget Sound that year, coinciding with cooler La Niña conditions—including increased upwelling—that provided more cool, saline water to the area in spring 2018 [84]. This local anomaly in cooler temperatures and lower disease further supports the notion that cooler temperatures suppress disease. In contrast, warmer spring temperatures could allow the pathogen to proliferate, causing disease outbreaks by the summer. Similar associations between June positive temperature anomalies and elevated disease were recently observed in intertidal eelgrass in the Northeast Pacific [9,32]. Based on these findings, spring temperatures could serve as an early indicator for summertime disease outbreaks.

Sites spanned environmental and latitudinal gradients and allowed us to measure disease across a broad spatial scale. Our results indicate widespread disease prevalence across all sites, and suggest that sites with severe infections could be at-risk for future declines. Further, they

indicate that even remote meadows with minimal human impacts, like Alaska and British Columbia, are at-risk for disease outbreaks. Since high-latitude meadows had lower disease compared to those at lower latitudes—and given that eelgrass ranges are expected to expand northward under climate change scenarios [46]—these northern meadows should be carefully monitored as potential refugia against disease and warm temperatures. A number of factorswere confounded with geographic region, including timing of sampling, latitude, and human impacts (ex: coastal development, water quality). While our study design could not partition the variation associated with these factors, these may be important in influencing wasting disease dynamics. For example, coastal urbanization could compromise eelgrass health, since nutrient enrichment from runoff triggers algal blooms and suspended sediments limit light, stressors that caused seagrass loss in an urban Florida estuary [85]. Future studies could target analyses on multiple wasting disease stressors.

Across regions and years, disease prevalence and severity were significantly lower in subtidal than intertidal meadows. When averaged across both years, disease severity was nearly three times lower in subtidal meadows, suggesting deeper habitats buffered the effects of environmental stressors and disease. Subtidal eelgrass may be more resilient and thus more resistant to wasting disease compared to intertidal eelgrass, and these deeper meadows could serve as refugia from future disease outbreaks and climate change conditions. This is consistent with findings that 20 years after mass eelgrass die-offs in the Chausey Archipelago, France, recovery was mostly limited to subtidal meadows [86]. Similar to terrestrial plants in environmental extremes [87], intertidal eelgrass that is exposed to highly variable environmental conditions at low tide—high and low temperatures, salinity, desiccation, UV stress [64]—may be more physiologically stressed and at-risk to infection compared to subtidal meadows, which are

not exposed at low tide and may be more disease-resilient. Similarly, deep temperate reefs act as refugia against marine heatwaves for habitat-forming corals, seaweeds, and eelgrass in Virginia and the Northeast Pacific, buffering against the harsh environmental conditions to which organisms at shallower depths are exposed [45,60–62,88].

Lower disease occurred in more dense eelgrass meadows and at cooler temperatures, regardless of tidal zone, but this association was more pronounced in intertidal meadows. However, this pattern is contrary to our hypothesis and disease theory, which would predict higher disease levels in high-density meadows, given that one of the mechanisms of seagrass wasting disease transmission is via direct contact between infected and healthy leaves [15]. Meadows with low eelgrass densities could have already experienced disease outbreaks or stressful conditions, leaving a reduced number of survivors with high disease prevalence and severity. Given that we observed strong interactions between temperature and density on disease prevalence, patchy meadows are likely more at-risk to synergies between thermal and disease stressors. Recent work corroborates similar findings on the resiliency of deeper eelgrass habitats, as deeper meadows had positive or neutral changes in eelgrass density following a marine heatwave, compared to significant declines in warmer, shallower meadows [45]. As such, high density eelgrass meadows under lower climate stress should be prioritized for conservation.

Generally, the mean densities, canopy heights, and leaf areas we observed were comparable to those in other eelgrass meadows in the Northeast Pacific [9,30,32]. The higher densities and reduced canopy heights and leaf areas in the San Juan Islands and Puget Sound, WA meadows are consistent with established differences in eelgrass growth patterns between tidal zones [89]. Intertidal and subtidal densities varied considerably, with orders of magnitude higher densities occurring at some sites compared to others in the same tidal zone. Densities

were more consistent in subtidal meadows year to year than intertidal meadows, further supporting our hypothesis that they are more environmentally stable and resilient against environmental disturbances; this is also reflected in lower disease in subtidal meadows. Our findings that leaf area and disease prevalence were significantly, positively associated also aligns with previous findings [9,29,30]. Based on leaf area alone and the usual association between disease and leaf size, subtidal meadows should have more disease, yet subtidal meadows consistently had reduced prevalence and severity. Again, this suggests greater resilience to disease of deeper, natural eelgrass meadows.

We specifically designed surveys to determine the association between temperature and disease in natural eelgrass meadows spanning the high biodiversity Northeast Pacific. Temperature is an important driver of historic and current wasting disease outbreaks worldwide [9,13,14,27,32,51]. Our machine-learning algorithm, EeLISA, enabled us to prioritize precise disease measurements and scale up our surveys. Field surveys that span broad, spatiotemporal scales are essential to tracking and predicting disease outbreaks in a rapidly changing ocean, and are needed to inform conservation and management decisions [90–92].

Connecting across scales from individuals, tidal zones, sites, and geographic regions, this large-scale field survey furthers our understanding of seagrass wasting disease dynamics in a changing ocean. Notably, it shows an association between reduced eelgrass disease, cooler temperatures, higher eelgrass densities, and deeper habitats. Our findings underscore a central need in managing marine resources in a rapidly warming climate: mapping resilient refugia. Surveys also reveal the conservation value of subtidal meadows as climate refugia. Though largely out of sight, expansive subtidal meadows cover more of Earth's surface area than intertidal meadows and create essential spawning habitat and nursery areas for innumerable fish

and other organisms [93]. This new indication of an important refuge from disease significantly increases the value of subtidal meadows, many of which are declining within the Salish Sea [9,68] and globally [39]. While previous field surveys compared wasting disease in eelgrass at different intertidal [9,29] and subtidal zones [31], no prior studies have compared disease between tidal zones. A relatively understudied aspect of wasting disease in eelgrass, these deeper refugia provide important opportunities for future conservation efforts.

This new information about lower wasting disease risk in cooler climates, cooler years, and deeper meadows can improve eelgrass management. First, to best inform conservation and preservation of these key habitats under mounting climate stress, continued monitoring of eelgrass meadows is essential, especially to monitor and track temperature-sensitive disease outbreaks. Intertidal meadows are most tractable for disease surveys, since they not only are easier to access from shore, but also have higher levels of disease, are more at risk, and may provide earlier warning of declines. Second, more protections should also be considered for both intertidal and subtidal meadows to buffer against future climate and disease-driven declines, especially in areas prone to more frequent, rapid warming with higher risk for disease outbreaks. Because subtidal meadows have the highest potential as safe havens against environmental and pathogenic stressors, eelgrass conservation activities should focus on protecting subtidal meadows. Given the increasing frequency and intensity of marine heatwaves [36,94] and other mounting environmental changes, understanding the synergistic effects of climate change and marine diseases on foundation species is critical to the sustainability of our oceans and planet [7].

Acknowledgements

We would like to thank our dedicated field research assistants who supported this project: Phoebe Dawkins, Coco Dawkins, James Lee, Miranda Winningham, Jack Novack, Carolyn Prentice, Tanya Prinzing, John Cristiani, Zach Monteith, Willem Weertman, Alex Lowe, Joey Ullman, Abigail Ames, Julia Kobelt, Christopher Wells, Maggie Shields, Wendel Raymond. We

would also like to thank Willem Weertman for making the ArcGIS map. Special thanks to Lillian Aoki, Maya Groner, Lynn Johnson, and Erika Mudrak for their invaluable statistical advice. Thanks to Nick Tolimieri for his instrumental support with Puget Sound fieldwork in summer 2017. The following generous funds supported this work: Cornell University's Atkinson Center for Sustainable Biodiversity Fund, Cornell Engaged Graduate Student Grant, Cornell Sigma Xi Research Grant, Andrew W. Mellon Student Research Grant, Dr. Carolyn Haugen, University of Washington Friday Harbor Labs Graduate Research Fellowship Endowment, Women Diver's Hall of Fame Scholarship in Marine Conservation to OJG; NSF-REU and Susan Lynch support for the Cornell Ocean Research Apprenticeship for Lynch Scholars to CK and SD; NSF awards OCE-1829921 and Washington SeaGrant (grant #NA18OAR4170095) to CB, Carolyn Friedman, CDH; NSF CompSustNet: Expanding the Horizons of Computational Sustainability (grant #1522054) to CG; Tula Foundation to OJG, EA, AO, MHL. The authors have no conflicts of interest to declare.

Data availability statement

All data and R scripts used to generate the analyses presented here will be publicly available via the Cornell University eCommons Repository by the time of publication (https://doi.org/10.7298/6ybh-w566).

References

1. Harvell CD, Mitchell C, Ward J, Altizer S, Dobson A, Ostfeld R, Samuel M. 2002 Climate Warming and Disease Risks for Terrestrial and Marine Biota. *Science* **296**, 2158–2162. (doi:10.1126/science.1063699)

2. Ward JR, Lafferty KD. 2004 The Elusive Baseline of Marine Disease: Are Diseases in Ocean Ecosystems Increasing? *PLoS Biol.* **2**, e120. (doi:10.1371/journal.pbio.0020120)

3. Tracy AM, Pielmeier ML, Yoshioka RM, Heron SF, Harvell CD. 2019 Increases and decreases in marine disease reports in an era of global change. *Proc. R. Soc. B Biol. Sci.* **286**, 20191718. (doi:10.1098/rspb.2019.1718)

4. Harvell CD. 1999 Emerging Marine Diseases--Climate Links and Anthropogenic Factors. *Science* **285**, 1505–1510. (doi:10.1126/science.285.5433.1505)

5. Harvell CD *et al.* 2019 Disease epidemic and a marine heat wave are associated with the continental-scale collapse of a pivotal predator (*Pycnopodia helianthoides*). *Sci. Adv.* **5**, eaau7042. (doi:10.1126/sciadv.aau7042)

6. Hobday AJ *et al.* 2016 A hierarchical approach to defining marine heatwaves. *Prog. Oceanogr.* **141**, 227–238. (doi:10.1016/j.pocean.2015.12.014)

7. Burge CA, Hershberger PK. 2020 Climate change can drive marine diseases. In *Marine Disease Ecology* (eds DC Behringer, BR Silliman, KD Lafferty), pp. 83–94. Oxford, United Kingdom: Oxford University Press.

8. Strydom S *et al.* 2020 Too hot to handle: Unprecedented seagrass death driven by marine heatwave in a World Heritage Area. *Glob. Change Biol.* **26**, 3525–3538. (doi:10.1111/gcb.15065)

9. Groner M *et al.* 2021 Warming sea surface temperatures fuel summer epidemics of eelgrass wasting disease. *Mar. Ecol. Prog. Ser.* (doi:https://doi.org/10.3354/meps13902)

10. Caldwell J, Heron S, Eakin C, Donahue M. 2016 Satellite SST-Based Coral Disease Outbreak Predictions for the Hawaiian Archipelago. *Remote Sens.* **8**, 93.

(doi:10.3390/rs8020093)

11. Harvell CD, Lamb JB. 2020 Disease outbreaks can threaten marine biodiversity. In *Marine Disease Ecology*, pp. 141–158. Oxford, United Kingdom: Oxford University Press.

12. Green E, Short F, editors. In press. *World Atlas of Seagrasses*. Berkeley, CA: University of California Press.

13. Martin DL, Chiari Y, Boone E, Sherman TD, Ross C, Wyllie-Echeverria S, Gaydos JK, Boettcher AA. 2016 Functional, Phylogenetic and Host-Geographic Signatures of Labyrinthula spp. Provide for Putative Species Delimitation and a Global-Scale View of Seagrass Wasting Disease. *Estuaries Coasts* **39**, 1403–1421. (doi:10.1007/s12237-016-0087-z)

14. Sullivan BK, Trevathan-Tackett SM, Neuhauser S, Govers LL. 2018 Review: Host-pathogen dynamics of seagrass diseases under future global change. *Mar. Pollut. Bull.* **134**, 75–88. (doi:10.1016/j.marpolbul.2017.09.030)

15. Muehlstein LK. 1992 The host – pathogen interaction in the wasting disease of eelgrass, *Zostera marina*. *Can. J. Bot.* **70**, 2081–2088. (doi:10.1139/b92-258)

16. Ralph P, Short F. 2002 Impact of the wasting disease pathogen, Labyrinthula zosterae, on the photobiology of eelgrass Zostera marina. *Mar. Ecol. Prog. Ser.* **226**, 265–271. (doi:10.3354/meps226265)

17. Pokorny KS. 1967 *Labyrinthula*. *J. Protozool.* **14**, 697–708. (doi:10.1111/j.1550-7408.1967.tb02065.x)

18. Short F, Mathieson A, Nelson J. 1986 Recurrence of the eelgrass wasting disease at the border of New Hampshire and Maine, USA. *Mar. Ecol. Prog. Ser.* **29**, 89–92. (doi:10.3354/meps029089)

19. Burdick D, Short F, Wolf J. 1993 An index to assess and monitor the progression of wasting disease in eelgrass Zostera marina. *Mar. Ecol. Prog. Ser.* **94**, 83–90. (doi:10.3354/meps094083)

20. Graham OJ, Aoki LR, Stephens T, Stokes J, Dayal S, Rappazzo B, Gomes CP, Harvell CD. 2021 Effects of Seagrass Wasting Disease on Eelgrass Growth and Belowground Sugar in Natural Meadows. *Front. Mar. Sci.* **8**, 768668. (doi:10.3389/fmars.2021.768668)

21. Renn C. 1936 The wasting disease of Zostera marina: A phytological investigation of the diseased plant. *Biol. Bull.* **70**, 148–158.

22. Short FT, Ibelings BW, Den Hartog C. 1988 Comparison of a current eelgrass disease to the wasting disease in the 1930s. *Aquat. Bot.* **30**, 295–304. (doi:10.1016/0304-3770(88)90062-9)

23. Stauffer RC. 1937 Changes in the Invertebrate Community of a Lagoon After Disapperance of the Eel Grass. *Ecology* **18**, 427–431. (doi:10.2307/1931212)

24. Moffitt J, Cottam C. 1941 Eelgrass depletion on the Pacific coast and its effect upon the Black Brant. , 26.

25. Milne L, Milne M. 1951 The eelgrass catastrophe. *Sci Am* **184**, 52–55.

26. Rasmussen E. 1977 The wasting disease of eelgrass (Zostera marina) and its effects on environmental factors and fauna. In *Seagrass Ecosystems: A Scientific Perspective* (eds CP McRoy, C Helfferich), pp. 1–52. New York: Marcel Dekker.

27. Bull JC, Kenyon EJ, Cook KJ. 2012 Wasting disease regulates long-term population dynamics in a threatened seagrass. *Oecologia* **169**, 135–142. (doi:10.1007/s00442-011-2187-6)

28. Bockelmann A-C, Tams V, Ploog J, Schubert PR, Reusch TBH. 2013 Quantitative PCR Reveals Strong Spatial and Temporal Variation of the Wasting Disease Pathogen, Labyrinthula zosterae in Northern European Eelgrass (Zostera marina) Beds. *PLoS ONE* **8**, e62169. (doi:10.1371/journal.pone.0062169)

29. Groner M *et al.* 2014 Host demography influences the prevalence and severity of eelgrass wasting disease. *Dis. Aquat. Organ.* **108**, 165–175. (doi:10.3354/dao02709)

30. Groner M, Burge C, Kim C, Rees E, Van Alstyne K, Yang S, Wyllie-Echeverria S, Harvell C. 2016 Plant characteristics associated with widespread variation in eelgrass wasting

disease. *Dis. Aquat. Organ.* **118**, 159–168. (doi:10.3354/dao02962)

31. Jakobsson-Thor S, Toth G, Brakel J, Bockelmann A, Pavia H. 2018 Seagrass wasting disease varies with salinity and depth in natural Zostera marina populations. *Mar. Ecol. Prog. Ser.* **587**, 105–115. (doi:10.3354/meps12406)

32. Aoki L. 2022 Disease surveillance using artificial intelligence links seagrass wasting disease to ocean warming across latitudes. In *Seagrass wasting disease: understanding host-pathogen interactions to ensure success in seagrass conservation and management*, Annapolis, MD.

33. Bos AR, Bouma TJ, de Kort GLJ, van Katwijk MM. 2007 Ecosystem engineering by annual intertidal seagrass beds: Sediment accretion and modification. *Estuar. Coast. Shelf Sci.* **74**, 344–348. (doi:10.1016/j.ecss.2007.04.006)

34. Schmidt AL, Wysmyk JKC, Craig SE, Lotze HK. 2012 Regional-scale effects of eutrophication on ecosystem structure and services of seagrass beds. *Limnol. Oceanogr.* **57**, 1389–1402. (doi:10.4319/lo.2012.57.5.1389)

35. Prentice C *et al.* 2020 A Synthesis of Blue Carbon Stocks, Sources, and Accumulation Rates in Eelgrass (*Zostera marina*) Meadows in the Northeast Pacific. *Glob. Biogeochem. Cycles* **34**. (doi:10.1029/2019GB006345)

36. Oliver ECJ *et al.* 2018 Longer and more frequent marine heatwaves over the past century. *Nat. Commun.* **9**, 1324. (doi:10.1038/s41467-018-03732-9)

37. Short FT, Kosten S, Morgan PA, Malone S, Moore GE. 2016 Impacts of climate change on submerged and emergent wetland plants. *Aquat. Bot.* **135**, 3–17. (doi:10.1016/j.aquabot.2016.06.006)

38. Smale DA *et al.* 2019 Marine heatwaves threaten global biodiversity and the provision of ecosystem services. *Nat. Clim. Change* **9**, 306–312. (doi:10.1038/s41558-019-0412-1)

39. Dunic JC, Brown CJ, Connolly RM, Turschwell MP, Côté IM. 2021 Long-term declines and recovery of meadow area across the world's seagrass bioregions. *Glob. Change Biol.* **27**, 4096–4109. (doi:10.1111/gcb.15684)

40. Kaldy JE. 2014 Effect of temperature and nutrient manipulations on eelgrass Zostera marina L. from the Pacific Northwest, USA. *J. Exp. Mar. Biol. Ecol.* **453**, 108–115. (doi:10.1016/j.jembe.2013.12.020)

41. Thom R, Southard S, Borde A. 2014 Climate-linked Mechanisms Driving Spatial and Temporal Variation in Eelgrass (Zostera marina L.) Growth and Assemblage Structure in Pacific Northwest Estuaries, U.S.A. *J. Coast. Res.* **68**, 1–11. (doi:10.2112/SI68-001.1)

42. Moore KA, Shields EC, Parrish DB. 2014 Impacts of Varying Estuarine Temperature and Light Conditions on Zostera marina (Eelgrass) and its Interactions With Ruppia maritima (Widgeongrass). *Estuaries Coasts* **37**, 20–30. (doi:10.1007/s12237-013-9667-3)

43. Ehlers A, Worm B, Reusch TBH. 2008 Importance of genetic diversity in eelgrass Zostera marina for its resilience to global warming. *Mar. Ecol. Prog. Ser.* **355**, 1–7. (doi:10.3354/meps07369)

44. Bintz JC, Nixon SW, Buckley BA, Granger SL. 2003 Impacts of temperature and nutrients on coastal lagoon plant communities. *Estuaries* **26**, 765. (doi:10.1007/BF02711987)

45. Magel CL, Chan F, Hessing-Lewis M, Hacker SD. 2022 Differential Responses of Eelgrass and Macroalgae in Pacific Northwest Estuaries Following an Unprecedented NE Pacific Ocean Marine Heatwave. *Front. Mar. Sci.* **9**, 838967. (doi:10.3389/fmars.2022.838967)

46. Wilson K, Lotze H. 2019 Climate change projections reveal range shifts of eelgrass Zostera marina in the Northwest Atlantic. *Mar. Ecol. Prog. Ser.* **620**, 47–62. (doi:10.3354/meps12973)

47. Kendrick GA *et al.* 2019 A Systematic Review of How Multiple Stressors From an Extreme Event Drove Ecosystem-Wide Loss of Resilience in an Iconic Seagrass Community. *Front. Mar. Sci.* **6**, 455. (doi:10.3389/fmars.2019.00455)

48. Orth RJ *et al.* 2006 A Global Crisis for Seagrass Ecosystems. *BioScience* **56**, 987. (doi:10.1641/0006-3568(2006)56[987:AGCFSE]2.0.CO;2)

49. Stevens NE. 1936 Environmental Conditions and the Wasting Disease of Eel-Grass. *Science*

682 **84**, 87–89. (doi:10.1126/science.84.2169.87)

683 50. Young E. 1943 Studies on Labyrinthula. The Etiologic Agent of the Wasting Disease of Eel-
684 Grass. *Am. J. Bot.* **30**, 586–593.

685 51. Lefcheck JS, Wilcox DJ, Murphy RR, Marion SR, Orth RJ. 2017 Multiple stressors threaten
686 the imperiled coastal foundation species eelgrass (*Zostera marina*) in Chesapeake Bay,
687 USA. *Glob. Change Biol.* **23**, 3474–3483. (doi:10.1111/gcb.13623)

688 52. Amon J. 1968 Studies Of Labyrinthula Spp In Culture. (doi:10.25773/V5-626Y-EJ81)

689 53. Dawkins P, Eisenlord M, Yoshioka R, Fiorenza E, Fruchter S, Giammona F, Winningham
690 M, Harvell C. 2018 Environment, dosage, and pathogen isolate moderate virulence in
691 eelgrass wasting disease. *Dis. Aquat. Organ.* **130**, 51–63. (doi:10.3354/dao03263)

692 54. Burge CA, Kim CJS, Lyles JM, Harvell CD. 2013 Special Issue Oceans and Humans Health:
693 The Ecology of Marine Opportunists. *Microb. Ecol.* **65**, 869–879. (doi:10.1007/s00248-013-
694 0190-7)

695 55. Dennison WC, Alberte RS. 1982 Photosynthetic responses of Zostera marina L. (Eelgrass) to
696 in situ manipulations of light intensity. *Oecologia* **55**, 137–144. (doi:10.1007/BF00384478)

697 56. Koch EW. 2001 Beyond Light: Physical, Geological, and Geochemical Parameters as
698 Possible Submersed Aquatic Vegetation Habitat Requirements. *Estuaries* **24**, 1.
699 (doi:10.2307/1352808)

700 57. Keppel G, Wardell-Johnson GW. 2012 Refugia: keys to climate change management. *Glob.*
701 *Change Biol.* **18**, 2389–2391. (doi:10.1111/j.1365-2486.2012.02729.x)

702 58. Keppel G, Van Niel KP, Wardell-Johnson GW, Yates CJ, Byrne M, Mucina L, Schut AGT,
703 Hopper SD, Franklin SE. 2012 Refugia: identifying and understanding safe havens for
704 biodiversity under climate change: Identifying and understanding refugia. *Glob. Ecol.*
705 *Biogeogr.* **21**, 393–404. (doi:10.1111/j.1466-8238.2011.00686.x)

706 59. Ellertsdottir E, Peters A. 1997 High prevalence of infection by endophytic brown algae in
707 populations of Laminaria spp. (Phaeophyceae). *Mar. Ecol. Prog. Ser.* **146**, 135–143.

60. Ladah LB, Zertuche-González JA. 2004 Giant kelp (Macrocystis pyrifera) survival in deep water (25–40 m) during El Niño of 1997–1998 in Baja California, Mexico. **47**, 367–372. (doi:10.1515/BOT.2004.054)

61. Van Oppen MJH, Bongaerts P, Underwood JN, Peplow LM, Cooper TF. 2011 The role of deep reefs in shallow reef recovery: an assessment of vertical connectivity in a brooding coral from west and east Australia: VERTICAL CONNECTIVITY IN A BROODING CORAL. *Mol. Ecol.* **20**, 1647–1660. (doi:10.1111/j.1365-294X.2011.05050.x)

62. Giraldo-Ospina A, Kendrick GA, Hovey RK. 2020 Depth moderates loss of marine foundation species after an extreme marine heatwave: could deep temperate reefs act as a refuge? *Proc. R. Soc. B Biol. Sci.* **287**, 20200709. (doi:10.1098/rspb.2020.0709)

63. Robertson AI, Mann KH. 1984 Disturbance by ice and life-history adaptations of the seagrassZostera marina. *Mar. Biol.* **80**, 131–141. (doi:10.1007/BF02180180)

64. Park SR, Kim S, Kim YK, Kang C-K, Lee K-S. 2016 Photoacclimatory Responses of Zostera marina in the Intertidal and Subtidal Zones. *PLOS ONE* **11**, e0156214. (doi:10.1371/journal.pone.0156214)

65. Zamora-Vilchis I, Williams SE, Johnson CN. 2012 Environmental Temperature Affects Prevalence of Blood Parasites of Birds on an Elevation Gradient: Implications for Disease in a Warming Climate. *PLoS ONE* **7**, e39208. (doi:10.1371/journal.pone.0039208)

66. Orth RJ, Heck KL, van Montfrans J. 1984 Faunal Communities in Seagrass Beds: A Review of the Influence of Plant Structure and Prey Characteristics on Predator: Prey Relationships. *Estuaries* **7**, 339. (doi:10.2307/1351618)

67. Hily C, Raffin C, Brun A, den Hartog C. 2002 Spatio-temporal variability of wasting disease symptoms in eelgrass meadows of Brittany (France). *Aquat. Bot.* **72**, 37–53. (doi:10.1016/S0304-3770(01)00195-4)

68. Christiaen B, Ferrier L, Dowty P, Gaeckle J, Berry H. 2022 Puget Sound Seagrass Monitoring Report, monitoring year 2018-2020.

69. Rappazzo BH, Eisenlord ME, Graham OJ, Aoki LR, Dawkins PD, Harvell D, Gomes C. 2021 EeLISA: Combating Global Warming Through the Rapid Analysis of Eelgrass Wasting Disease. , 10.

70. Groner ML *et al.* 2018 Oysters and eelgrass: potential partners in a high pCO_2 ocean. *Ecology* **99**, 1802–1814. (doi:10.1002/ecy.2393)

71. JPL 2015. In press. GHRSST Level 4 MUR Global Foundation Sea Surface Temperature Analysis.

72. R Core Team. 2020 R: A language and environment for statistical computing.

73. Neuwirth, E. 2014 RColorBrewer: ColorBrewer Palettes. R package version 1.1-2.

74. Wickham H. 2016 *ggplot2: Elegant Graphics for Data Analysis.* New York: Springer-Verlag.

75. Kassambara A. 2020 ggpubr: 'ggplot2' Based Publication Ready Plots.

76. Zuur AF, Ieno EN. 2016 A protocol for conducting and presenting results of regression-type analyses. *Methods Ecol. Evol.* **7**, 636–645. (doi:10.1111/2041-210X.12577)

77. Brooks M, Kristensen K, van Benthem K, Magnusson A, Berg C, Nielsen A, Skaug H, Maechler M, Bolker B. 2017 glmmTMB Balances Speed and Flexibility Among Packages for Zero-inflated Generalized Linear Mixed Modeling. *R J.* **9**, 378–400.

78. Bates D, Maechler M, Bolker B, Walker S. 2015 Fitting Linear Mixed-Effects Models Using lme4. *J. Stat. Softw.* **67**, 1–48. (doi:10.18637/jss.v067.i01)

79. Beca-Carretero P, Stanschewski CS, Julia-Miralles M, Sanchez-Gallego A, Stengel DB. 2019 Temporal and depth-associated changes in the structure, morphometry and production of near-pristine Zostera marina meadows in western Ireland. *Aquat. Bot.* **155**, 5–17. (doi:10.1016/j.aquabot.2019.02.003)

80. Hartig F. 2021 DHARMa: Residual Diagnostics for Hierarchical (Multi-Level/Mixed) Regression Models.

81. Warton DI, Hui FKC. 2011 The arcsine is asinine: the analysis of proportions in ecology. *Ecology* **92**, 3–10. (doi:10.1890/10-0340.1)

82. Ludecke D. 2021 sjPlot: Data Visualization for Statistics in Social Science.

83. Menning DM, Gravley HA, Cady MN, Pepin D, Wyllie-Echeverria S, Ward DH, Talbot SL. 2021 Metabarcoding of environmental samples suggest wide distribution of eelgrass (Zostera marina) pathogens in the north Pacific. *Metabarcoding Metagenomics* **5**, e62823. (doi:10.3897/mbmg.5.62823)

84. Newton J, Mickett J, Manalang D, Carini R. 2022 Salish Sea ORCA buoy observations over the last decade: Warmer and saltier than normal anomalies and their persistence. Poster presented at the Salish Sea Ecosystem Conference.

85. Lapointe BE, Herren LW, Brewton RA, Alderman PK. 2020 Nutrient over-enrichment and light limitation of seagrass communities in the Indian River Lagoon, an urbanized subtropical estuary. *Sci. Total Environ.* **699**, 134068. (doi:10.1016/j.scitotenv.2019.134068)

86. Godet L, Fournier J, van Katwijk M, Olivier F, Le Mao P, Retière C. 2008 Before and after wasting disease in common eelgrass Zostera marina along the French Atlantic coasts: a general overview and first accurate mapping. *Dis. Aquat. Organ.* **79**, 249–255. (doi:10.3354/dao01897)

87. Lucas GB, Campbell CL, Lucas LT. 1992 Causes of Plant Diseases. In *Introduction to Plant Diseases: Identification and Management* (eds GB Lucas, CL Campbell, LT Lucas), pp. 9–14. Boston, MA: Springer US. (doi:10.1007/978-1-4615-7294-7_2)

88. Aoki LR, McGlathery KJ, Wiberg PL, Al-Haj A. 2020 Depth Affects Seagrass Restoration Success and Resilience to Marine Heat Wave Disturbance. *Estuaries Coasts* **43**, 316–328. (doi:10.1007/s12237-019-00685-0)

89. Larkum AWD, Orth RJ, Duarte CM, editors. 2006 *Seagrasses: biology, ecology, and conservation*. Dordrecht, The Netherlands: Springer.

90. Anderson PK, Cunningham AA, Patel NG, Morales FJ, Epstein PR, Daszak P. 2004

Emerging infectious diseases of plants: pathogen pollution, climate change and agrotechnology drivers. *Trends Ecol. Evol.* **19**, 535–544. (doi:10.1016/j.tree.2004.07.021)

91. Altizer S, Ostfeld RS, Johnson PTJ, Kutz S, Harvell CD. 2013 Climate Change and Infectious Diseases: From Evidence to a Predictive Framework. *Science* **341**, 514–519. (doi:10.1126/science.1239401)

92. Groner ML *et al.* 2016 Managing marine disease emergencies in an era of rapid change. *Philos. Trans. R. Soc. B Biol. Sci.* **371**, 20150364. (doi:10.1098/rstb.2015.0364)

93. Heck K, Hays G, Orth R. 2003 Critical evaluation of the nursery role hypothesis for seagrass meadows. *Mar. Ecol. Prog. Ser.* **253**, 123–136. (doi:10.3354/meps253123)

94. Meehl GA. 2004 More Intense, More Frequent, and Longer Lasting Heat Waves in the 21st Century. *Science* **305**, 994–997. (doi:10.1126/science.1098704)

Figure Captions

Figure 1. (A) Locations for seagrass wasting disease surveys in Alaska, British Columbia, San Juan Islands, and Puget Sound in summers 2017 and 2018. Surveys included paired subtidal and intertidal eelgrass meadows. Map made in ArcGIS. (B) Site-level disease severity reflect lower disease in subtidal meadows and generally higher disease in 2018; n=5761 blades (mean ± SE). Sites are arranged north to south, top to bottom within and by regions. Sites with missing bars did not have eelgrass and do not represent that there was not any disease present (intertidal: Triquet N, Choked; subtidal: Hakai).

Figure 2. (A) Correlations between measured March cumulative negative temperature anomaly and measured transect-level disease prevalence in intertidal and subtidal meadows. Bands represent 95% CI. Temperature anomalies are centered and scaled. Also shown are representative eelgrass in (B) intertidal and (C) subtidal meadows. Image E credit: A Hausner.

Figure 3. (A) Cumulative March negative sea surface temperature anomalies in 2017 and 2018. Cooler temperatures in 2018 in Puget Sound (PS) corresponded with lower disease levels that year. (B) Predicted disease prevalence in 2017 and 2018 given observed cumulative March negative temperature anomalies and mean, scaled leaf area. Predictions are based on the leaf-level prevalence model in Table S3. Bands represent 95% confidence intervals. Temperature anomalies are centered and scaled.

818

819

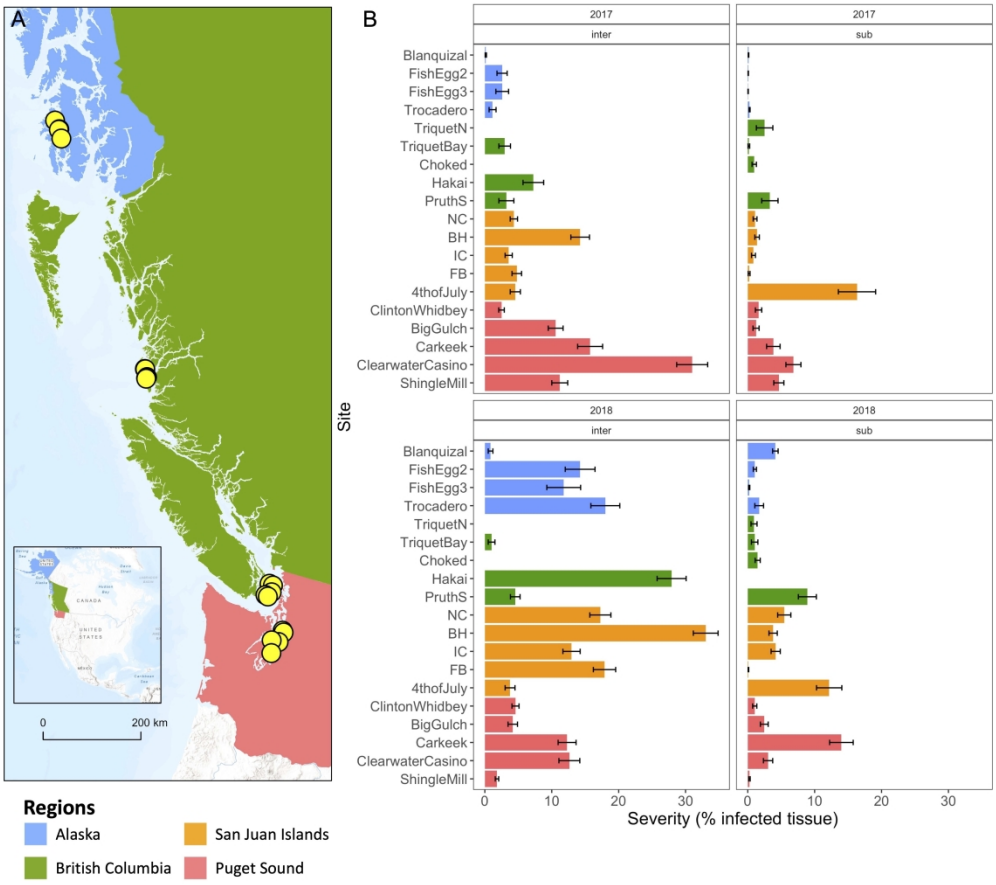

Figure 1. (A) Locations for seagrass wasting disease surveys in Alaska, British Columbia, San Juan Islands, and Puget Sound in summers 2017 and 2018. Surveys included paired subtidal and intertidal eelgrass meadows. Map made in ArcGIS. (B) Site-level disease severity reflect lower disease in subtidal meadows and generally higher disease in 2018; n=5761 blades (mean ± SE). Sites are arranged north to south, top to bottom within and by regions. Sites with missing bars did not have eelgrass and do not represent that there was not any disease present (intertidal: Triquet N, Choked; subtidal: Hakai).

1587x1410mm (72 x 72 DPI)

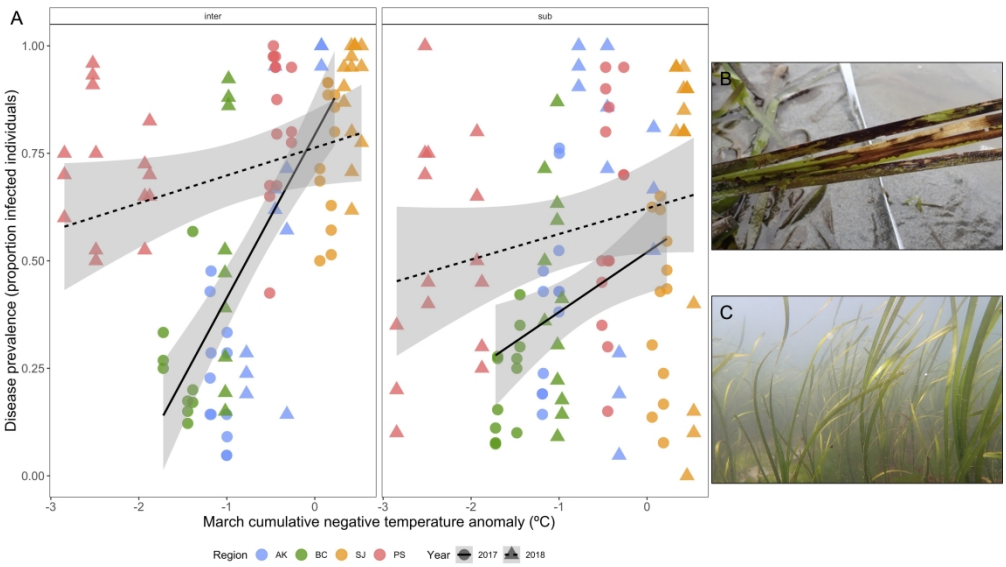

Figure 2. (A) Correlations between measured March cumulative negative temperature anomaly and measured transect-level disease prevalence in intertidal and subtidal meadows. Bands represent 95% CI. Temperature anomalies are centered and scaled. Also shown are representative eelgrass in (B) intertidal and (C) subtidal meadows. Image E credit: A Hausner.

2822x1587mm (72 x 72 DPI)

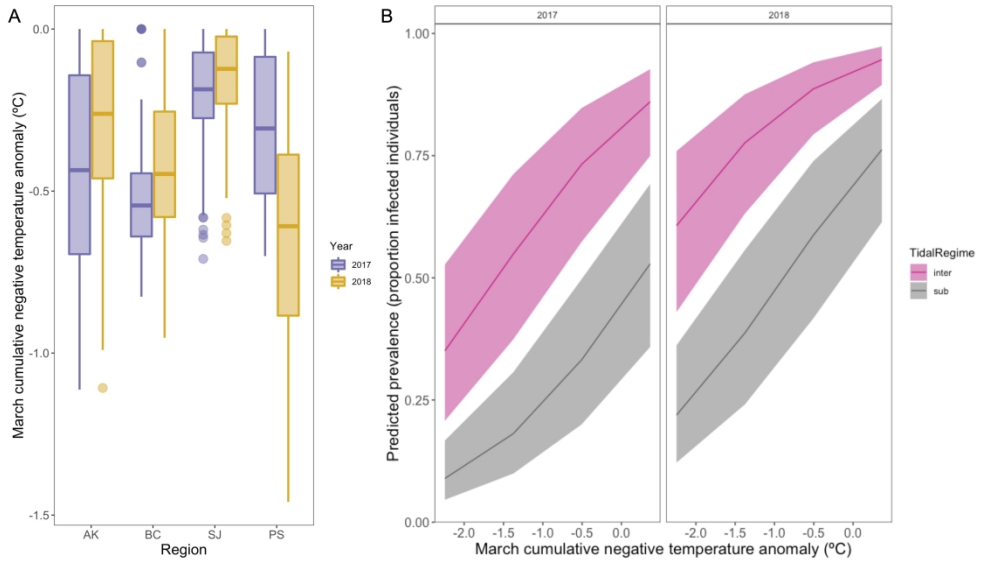

Figure 3. (A) Cumulative March negative sea surface temperature anomalies in 2017 and 2018. Cooler temperatures in 2018 in Puget Sound (PS) corresponded with lower disease levels that year. (B) Predicted disease prevalence in 2017 and 2018 given observed cumulative March negative temperature anomalies and mean, scaled leaf area. Predictions are based on the leaf-level prevalence model in Table S3. Bands represent 95% confidence intervals. Temperature anomalies are centered and scaled.

2822x1587mm (72 x 72 DPI)